INHERENT MECHANISM OF BREAKDOWN IN LAMINAR-TURBULENT TRANSITION

H. Zhou [hzhou1@tju.edu.cn]
Department of Mechanics, Tianjin University; Liu-Hui center of Applied Mathematics, Nankai and Tianjin University. Tianjin 300072, China

ABSTRACT: The most obvious manifestation of the breakdown process in laminar-turbulent transition is the catastrophic change of its mean flow profile from laminar to turbulent. Here we show by analyzing the results from direct numerical simulations that the key effect leading to this change is the drastic change of stability characteristics of the mean flow profile during the breakdown process. This mechanism works for both incompressible and compressible flows.

1. INTRODUCTION

The most obvious differences between turbulent and laminar flows are: (1) their mean flow profiles; (2) the laminar flow is regular, while the turbulent flow is irregular, or random.

From hydrodynamic stability theory point of view, the laminar flow profile can support unstable eigen-mode solution when the Reynolds number is sufficiently large. The eigen-function bears a global character in the sense that the solution spans the whole region of the flow in the direction normal to the flow.

Contrary to that, the mean flow profile of turbulent flow does not support global unstable eigen-mode solution. For wall bounded turbulent flows such as plane channel flow and boundary layer flow, there are two distinct regions in the flow, namely, the wall region and the outer region. The investigation by Tsujimoto and Miyake showed that the wall region has its own dynamics [1], which manifests itself as the generation of coherent structures, by which turbulent energy is extracted from the mean flow, and then by the so-called bursting and sweeping, turbulent energy was brought to the outer region. On the other hand, it needs some sort of disturbances from the outer region to trigger the initial disturbances for the generation of coherent structures.

Coherent structures are essentially generated due to some sort of instability of the flow in the wall region, as shown by Zhou et al's models [2-6], which bears a strong local nature in the sense that the disturbance velocity induced by the coherent structures decays very fast outside the wall region. Thus, wall bounded turbulent flows are essentially maintained by the interactions of disturbances in the wall region with those in the outer region, and the outer region plays a relatively passive role. The existence of distinct wall and outer regions is obviously the consequence of mean flow modification.

The essential mechanism for laminar-turbulent transition must be a mechanism leading to quick modification of the mean flow. So far, existing theories do not provide such a mechanism.

The method of our investigations were that, first, direct numerical simulations were done for laminar-turbulent transitions, then followed by analysis of the results.

2. CASES FOR INCOMPRESSIBLE FLOWS

Plane channel flow was taken as the prototype for investigation. The initial flow field was a parabolic laminar flow superimposed with three T-S waves expressed as follows:

$$a_1\mathbf{u}_1(y)e^{i(\alpha_1 x+\beta_1 z)} + a_2\mathbf{u}_2(y)e^{i(\alpha_2 x+\beta_2 z)} + a_3\mathbf{u}_3(y)e^{i(\alpha_3 x+\beta_3 z)} \qquad (1)$$

where x, y, x are coordinates in the stream-wise, normal-wise and span-wise directions respectively; α_i and β_i (i=1,2,3), the wave numbers in x and z directions respectively; $\mathbf{u}_i$ (i=1,2,3), the eigen-velocity vectors solved from the eigen-value problem of Orr-Sommerfeld equation for the laminar profile, normalized by the condition that $\max|u_i| = 1$, where u_i is the stream-wise velocity component; and a_1, a_2, a_3 the amplitudes. Details of numerical method can be found elsewhere [7].

Altogether, six cases were computed, their parameters are shown in Table 1, in which the Reynolds number Re was based on the center velocity of the laminar flow and the half channel width. The first five cases belonged to regular transition, for which the breakdown was preceded by gradual amplification of disturbances. The last case belonged to by-pass transition, for which there was no gradual amplification of disturbances preceding the breakdown. But no matter which categories they belonged to, their breakdown processes underwent similar route, hence here we show only results for case 1.

Table 1: Parameters for cases studied

	α_1	β_1	α_2	β_2	α_3	β_3	a_1	a_2	a_3	Re
Case 1	1.0	0	0.8	0.6	1.0	0.3	0.002	0.002	0.002	8000
Case 2	1.0	0	0.8	0.6	1.0	0.3	0.002	0.002	0.002	7000
Case 3	1.0	0	0.8	0.6	1.0	0.3	0.08	0.08	0.01	8000
Case 4	2.1	0	1.5	0.9	1.5	0.3	0.08	0.08	0.01	7000
Case 5	2.7	0	2.1	0.9	1.5	0.3	0.08	0.08	0.01	7000
Case 6	1.0	0	0.8	0.6	1.0	0.3	0.18	0.18	0.18	8000

The disturbances evolved gradually at first and kept quite regular until about t=340, as shown in Fig. 1a, in which the velocity component u at a certain point induced by the Fourier components having the same wave numbers as the second input wave is shown. Fig. 1b shows that the mean flow profile was still very close to the parabolic profile up to this moment, and Fig. 1c shows that the mean velocity gradient at the wall started to increase sharply after t=340.

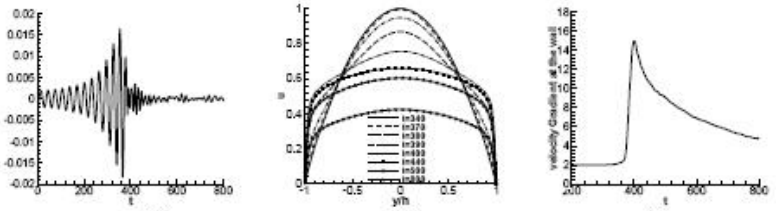

Fig.1: (a) velocity u of a certain point induced by the wave with wave numbers α_2 and β_2, (b) Mean flow profiles at different times, (c) time history of mean velocity gradient at the wall

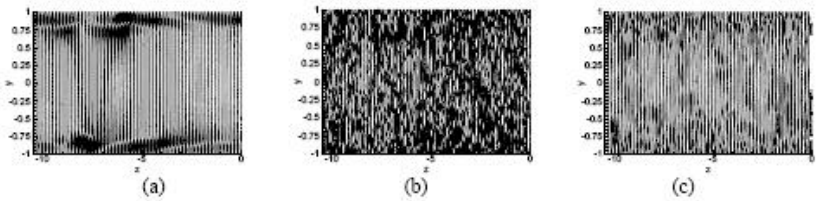

Fig. 2: Velocity vector plots in a certain y-z plane. (a) t=340, (b) t=400, (c) t=800.
The vector length in (a) has been enlarged by a factor of 3

Fig. 2 shows the velocity vector plot in a certain y-z plane at t=340, 400 and 500, corresponding to time instants before, during and after the breakdown process respectively. For t=340, the disturbance was

still quite regular, having a global nature as noted before. For t=400, the disturbances already spread over the whole plane, implying that many more harmonics were excited. For t=800, disturbances manifested mainly as vortices, or coherent structures, near the two walls without mutual correlations, which is typical for turbulent flows. Fourier analysis also revealed that many more harmonics were quickly excited during the breakdown process, and their amplitudes were even bigger than those for fully developed turbulence.

Although at t=800, the breakdown process has already been accomplished, as the shape of the mean flow profile already resembles the turbulent profile and the mean velocity gradient at the wall has already decreased sharply from its peak value, but it was still far from the final equilibrium state of turbulence. Because, for the equilibrium turbulent flow, the maximum velocity of the mean flow should be close to 0.28 for R=8000, and the mean velocity gradient at the wall should be 0.5, the same as the laminar flow, as we used the constant pressure gradient formulation for our numerical simulation. The slowness of the mean flow in approaching its final equilibrium state is due to the fact that the mean flow modification is governed by a diffusion equation with a small coefficient for its diffusive term. But during the breakdown process, its modification was very quick due to the largeness of the disturbance, as manifested in Fig.2b.

The above result includes a previously unknown fact that during breakdown, many more harmonics were greatly enhanced, not only compared with those before transition, but also compared with those after transition. This is just the reason why the breakdown process could bears a certain catastrophic nature. Naturally, it poses a question, what is the key mechanism leading to the quick enhancement of many harmonics during breakdown? Simply refer to non-linear interaction seems is not adequate.

Figure 1 shows that the mean flow profile started to have appreciable change at t=370, manifesting in the appearance of slight inflection points. We analyzed the linear stability characteristics of the mean flow profiles for several time instants during the breakdown process, corresponding to t=375, 380, 385 and 390 respectively. Their neutral curves in α and β plane, together with those for the original parabolic profile, were shown in Fig.3. Compared with the one for the parabolic profile, the unstable zones encircled by the neutral curves were drastically enlarged, and their maximum amplification rates were also significantly increased to 0.00507, 0.01570, 0.01552 and 0.01791 respectively, compared with 0.002735 for the laminar profile. We claim that the enlargement of the unstable zone and the significant increase of the amplification rate were the only possible basis for the quick generation and enhancement of many harmonics, resulting in the quick modification of the mean flow profile. Such a quick generation and enhancement of many harmonics could not be explained by simply refer to non-linear interactions among different harmonics.

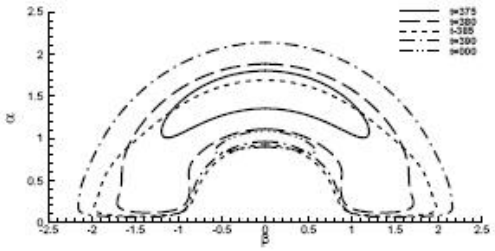

Fig. 3: Neutral curve in α, β plane. t=000 corresponds to laminar profile.

Judging by the mean flow profile in Fig.1b, one can see that the breakdown process started from sometime between t=340 to 370, when it started to deviate from the original parabolic profile, and the process practically ended at sometime between t=400 to 440, when the profile already bore the typical shape of turbulent profile that its central part became flat. The total time of transition was of the order of 40-50 time units.

As mentioned earlier, among the six cases investigated, the first five belonged to regular transition, while the last one belonged to by-pass transition, but their breakdown process all underwent similar sequence of mean flow profile modifications. The only difference was that for the last case, because of its large initial amplitudes, the modification of the mean flow profile took place immediately without going through a process of gradual amplification of the initial disturbances and the breakdown process took less time. But still, its stability characteristics underwent similar sequence of changes, just like other cases.

Laminar-turbulent transition for boundary layers has also been studied, and the conclusion was the same.

3. CASES FOR SUPERSONIC BOUNDARY LAYERS

Mack (1984) [8] found that, by linear stability theory, different from incompressible flow, there were more than one unstable wave modes for supersonic boundary layers when the Mach number exceeded 2, and the maximum amplification rate for second mode became larger than those for the first mode when the Mach number exceeded about 4. Mack's finding was confirmed by experiment of Stetson and Kimmel (1992) [9]. Experimental data for transition were rare. Bountin et al (2001) [10] confirmed the existence of the second mode disturbances, but transition was determined by the first mode disturbances. Malik (2003) [11] analyzed the transition data from two different hypersonic flight tests, and found that the transition in both cases was caused by the amplification of second mode disturbances. Their statements seem to be not very consistent, but all of them were concerned only with the evolution of disturbances before the breakdown process, not during the breakdown process itself.

The existence of more than one unstable wave modes for supersonic flows makes it more complicated for its transition investigation.

The evolution of disturbances in a supersonic boundary layer is obviously of spatial mode. However, direct numerical simulation for transition in spatial mode needs much more computer resources, at least one order larger than its counterpart in temporal mode. We have carried out both kinds of simulations. But for temporal mode, the computational results were much more comprehensive, and we did find that the breakdown process in both cases were very similar, hence in what follows, only results obtained from temporal mode simulation were presented.

Details of numerical method can be found elsewhere [12].

Transition of a supersonic boundary layer on a flat plate with a Mach number 4.5 was studied. The Reynolds number Re_δ, for which the reference length was the displacement thickness of the laminar boundary layer at 2.2m downstream of the leading edge, was 17000.

The initial condition was the similarity solution with local parallel assumption superimposed with three T-S waves, similar to those for incompressible flows as expressed in equ.(1). The only difference was now $\mathbf{u}_j$ has five components as $\mathbf{u}_j=(u,v,w,T,p)$, where T was the temperature, and p the pressure.

Similarity solution with parallel assumption was obviously not an exact stationary solution of N-S equation. To make it so, a small steady source term was added to the N-S equations. Similar method has also been used elsewhere, see for example Dinavahi et al (1994) [13].

As stated above, for a laminar supersonic boundary layer on a flat plate with Mach number 4.5, there exist two unstable modes of T-S waves, namely the first mode and the second mode. In Fig.4 (a) and (b) are the neutral curves for both modes in (α,β) plane and max $|\omega_i|$ vs. β for the laminar flow profile. It can be seen that the maximum amplification rates for the first mode waves was smaller than those for the second mode waves, and a two-dimensional second mode wave had the largest amplification rate. Eigen-functions of most unstable two-dimensional waves for both modes were shown in Fig.4 (c) and (d) respectively. Notice that the locations for the peaks of u, v eigen-functions of the second mode wave were much closer to the wall than their counterparts for the first mode wave. So the second mode wave mainly modifies the velocity mean flow profile in a region near the wall, while the first mode wave could modify the velocity mean flow profile in a much larger region, not restricted in a region near the wall. Hence, the ability of modifying the mean flow profile was different for the two modes.

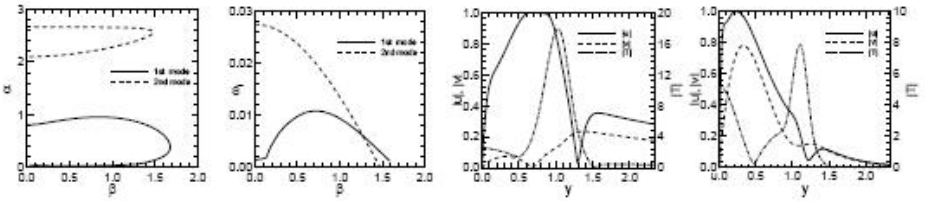

Fig.4: For laminar flow: (a) Neutral curve in (α,β) plane, (b) max ω_i vs. β, (c) eigen-functions for first mode T-S wave 1, (d) eigen-functions for second mode T-S wave.

Two different initial disturbances have been chosen, and their parameters were shown in Table2. The three waves in case A and B were of second mode and first mode respectively.

Table 2: Disturbance parameters for cases studied

Case	n	a	A	β	Ω
A	1	0.05	2.625	0.0	(2.352 452 00, 0.007 797 90)
	2	0.05	2.625	0.5	(2.357 698 00, 0.007 218 90)
	3	0.05	2.1	1.0	(2.036 365 00,-0.014 281 90)
B	1	0.01	0.6	0.0	(0.500 870 76, 0.001 437 41)
	2	0.01	0.4	0.6	(0.313 292 73, 0.009 846 81)
	3	0.01	0.4	0.8	(0.316 863 06, 0.010 735 44)

For the case A, the evolution curves for the average skin-friction coefficient C_f, and the disturbance energy e2 were shown in Fig. 5(a). In Fig.5 (b) and (c) were the time history of the velocity component u at a certain point induced by the Fourier components with wave numbers (2.625,0.0) and (2.1,1.0). One can see that the disturbances became irregular at about t=120, which should be the beginning of the breakdown process. This moment coincided with the starting point of the sharp increase of the skin-friction coefficient. The transition process ended practically at the time when the skin friction coefficient took its peak value.

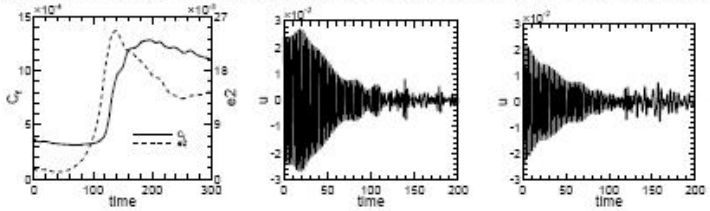

Fig.5: Time history of: (a) skin-friction coefficient C_f and disturbance energy, (b) and (c) velocity u of a certain point induced by wave with wave number (2.625,0.0) and (2.1,1.0) respectively.

It can be seen from Fig.6 (a) and (b), showing the mean flow profiles of velocity u and density ρ at different times, that the mean flow profiles underwent rapid modification in the time interval [100, 200] and a slight inflexion point appeared for the profiles of at t=100 and t=125. In the time interval [200,300], the mean flow profile of velocity already changed slowly, but the mean flow profile of density still had relatively rapid change, indicating that the fully developed state of turbulence has not been reached yet at

this moment. Fig.6 (c) and (d) show the velocity vector plot in a certain y-z plane at t=60 and t=200 respectively. At t=60, the disturbances were still quite regular, while at t=200, the disturbances were greatly amplified and spread over entire boundary layer, implying that many more harmonics were excited and enhanced.

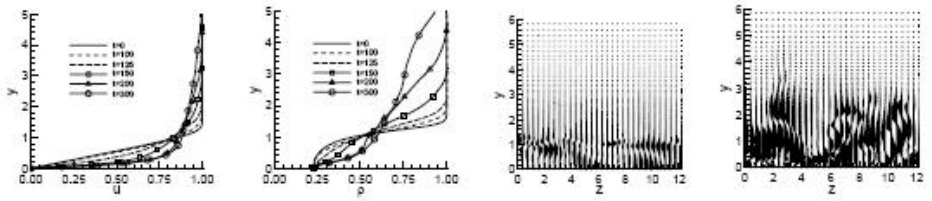

(a) (b) (c) (d)

Fig.6: Mean flow profiles at different time instants. (a) velocity u, (b) density ρ; velocity vector plots in a certain y-z plane, (c) t=60, (d) t=200 (the vector length of (c) has been enlarged by a factor 3).

By linear stability analysis, neutral curves for the mean flow profile were computed for five different time instants, i.e. t=0, 125, 130, 135 and 140. Neutral curves in (α,β) plane and max ω_i vs. β for both first and second modes T-S waves were shown in Fig.7. Because it was symmetric with respect to α axis, only those parts corresponding to β≥0 were shown. The unstable zones encircled by the neutral curves of first mode were drastically enlarged, and their respect maximum amplification rates were also significantly increased, from 0.01 at t=0 for laminar flow profile, to 0.03, 0.025 and 0.024 respectively for later time instants. On the contrary, the unstable zones of second mode decreased gradually and totally disappeared after t=135, and the corresponding maximum amplification rate also decreased gradually from 0.027 until to a negative value. The implication was that, although the three initial disturbance waves were of the second mode, their effect decreased progressively during the breakdown process when the mean flow profile was being modified. At the same time, the effect of first mode disturbance waves became more and more important. In fact, only first mode disturbance waves were able to modify effectively the mean profile of laminar flow beyond the laminar boundary layer thickness, leading to thickness increase and finally became the turbulent mean flow profile.

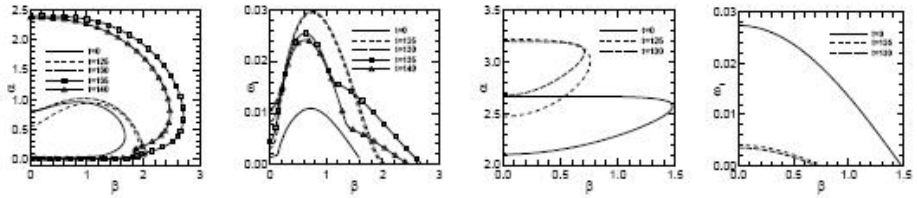

(a) (b) (c) (d)

Fig.7: (a) Neutral curves of first mode T-S waves in (α,β) plane at different time instants, (b) corresponding max ω_i vs. β for first mode T-S waves, (c) Neutral curves of second mode T-S waves in (α,β) plane at different time instants, (d) corresponding max ω_i vs. β for second mode T-S waves.

Evolution curves of the amplitude of velocity u induced by waves with wave number (0.525, 1.5) and (2.625, 1.0), corresponding to first and second mode unstable waves respectively, were shown in Fig.8(a). The amplitude of second mode unstable wave remained relatively small in the whole course and even decayed gradually after the beginning of breakdown process. On the other hand, the first mode

unstable wave increased rapidly after being excited until about t=160, reaching its maximum amplitude 0.035 and remained to be about 0.015 after breakdown, further indicating that the unstable wave of the first mode played a key role in the breakdown process.

Fig.5 (a) showed that there was a sharp increasing of skin-friction coefficient between t=125 and t=150, eigen-functions with wave number (0.525, 1.5) of first mode corresponding to these two time instants were shown in Fig.8 (b) and (c). The y direction extent where the eigen-function took relatively large value expanded appreciably from t=125 to t=150, even beyond the original laminar boundary layer thickness, thus providing the mechanism for the rapid mean flow profile modification not only near the wall, but also outside the original laminar boundary layer.

On the contrary, as was shown in Fig.8 (a), the amplitude of the second mode wave reached its peak value at about t=60, while Fig.6 (a) and (b) showed that the mean profile of velocity u and density ρ remained almost unchanged near the wall until up to t=100, implying that the second mode unstable wave did not play a key role in the breakdown process of transition.

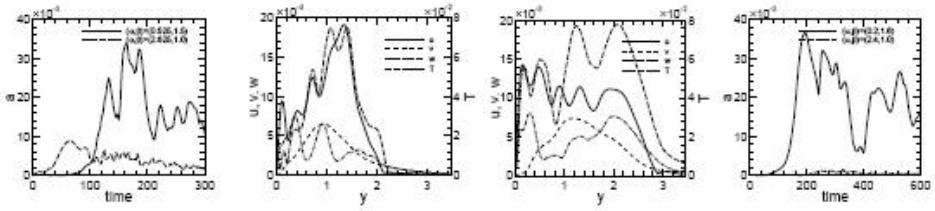

Fig.8: (a) Amplitude of velocity u induced by wave with wave number (α,β), (b) eigen-functions of first mode wave with wave number (0.525, 1.5) at t=125, (c) eigen-functions of first mode wave with wave number (0.525, 1.5) at t=150, (d) amplitude of velocity u induced by wave with wave number (α,β) for case B.

The breakdown process in case B was similar to case A, except it took a somewhat longer time for its accomplishment. Evolution curves for the amplitude of velocity u induced by first mode wave with wave number (0.2, 1.6) and second mode wave with wave number (2.4, 1.0) were shown in Fig. 8(d). Again the amplitude of the second mode unstable wave was very small, so the first mode unstable wave played the key role in breakdown.

4. DISCUSSIONS

One can summarize the breakdown process as follows: when the disturbances become larger, harmonics will be generated through non-linear interaction, and the mean flow profile will also be modified. At a certain stage, which is crucial for the breakdown, the stability characteristics of the mean flow profile starts to have drastic change due to the modification, manifesting in the much enlarged unstable zone in the wave number plane and the significant increase of the amplification rates. Only under such circumstance, many more harmonics can be generated and enhanced very quickly, which in turn lead to further quick modification of the mean flow profile, resulting in the catastrophic change of the mean flow profile and ended with a turbulent flow.

It is interesting to note that to make the laminar flow profile starts to be modified noticeably in the sense that its stability characteristics starts to have noticeable change, the amplitude of disturbance should be of the order 0.01. In the nonlinear theory of hydrodynamic stability, there are several mechanisms being thought to be the main causes leading to transition, notably, the secondary instability, the resonant triad, etc. However, investigations showed that only when the amplitude of the primary wave reach a magnitude of

the order 0.01, then the amplification rate of the secondary instability wave could exceed the maximum amplification rate of the T-S waves, meaning that the mechanism of secondary instability is meaningful only under this condition. The same is true for the resonant triad mechanism. While under the same condition, the mechanism suggested in this paper also starts to work. In fact, from our numerical simulations for incompressible flows, we found that if the initial disturbance amplitudes were small, then the breakdown processes all started at a moment when the amplitude of the largest disturbance wave was of the order 0.01–0.02, and no sign of secondary instability or resonant triad was found. Besides, mechanism of secondary instability and resonant triad work only in carefully controlled experiments, so perhaps their importance was overestimated.

ACKNOWLEDGEMENT

Works relevant to this paper were supported by foundation items: the National Natural Science Foundation of China (90205021); FANEDD (200328), and were also partially support by Liu Hui Center of Applied Mathematics, Nankai University and Tianjin University, and most of them were done by my colleagues, Prof. Ji-sheng Luo, Prof. Wei Cao, and students, Mr. Xing-jun Wang, Mr. Zhang-feng Huang, to them I am most grateful.

REFERENCES

[1] Tsujimoto, K. & Miyake, Y. Universal property of autonomous layer in near-wall turbulence, IUTAM Symposium on Geometry and Statistics of Turbulence, Kluwer Academic Publication, editors: T. Kambe et al., 385-390, (2001)

[2] Zhou, H., Xiong, Z., The mechanism for the geration of coherent structures in the wall region of a turbulent boundary layer, Science in China (Series A), **38** (2): 188-198, (1995)

[3] Zhou, H., Coherent Structure Modeling and its Role in the Computation of Passive Quantity Transport in Turbulent Boundary Layer, JSME International Journal, Series B, **41**(1): 137-144, (1998)

[4] Zhou, H., Lu, C., Luo, J., Modeling of individual coherent structures in the wall region of a turbulent boundary layer, Science in China (Series A), **42** (6): 627-635, (1999)

[5] Zhang Dongming, Luo Jisheng, Zhou Heng, Dynamic model of coherent structure in the wall region of a turbulent boundary layer, Science in China (Series G), **46**(3), 291-299, (2003)

[6] ZHANG Dong-ming, LUO Ji-sheng, ZHOU Heng, A mechanism for excitation of coherent structures in the wall region of a turbulent boundary layer, Applied Mathematics and Mechanics, 2005, **26**(4), 415-422

[7] Luo J S, Wang X J, Zhou H. Inherent mechanism of breakdown in laminar-turbulent transition of plane channel flows. *Science in China, Ser G*, 2005, **48**(2):228~236

[8] Mack L M. Boundary layer linear stability theory. In *AGARD Rep*, 1984, 709.

[9] Stetson K F and Kimmel R L. On hypersonic boundary layer stability. AIAA-92-0737.

[10] Bountin D A, Sidorenko A A, and Shiplyuk A N. Development of natural disturbances in a hypersonic boundary layer on a sharp cone. *Journal of Applied Mechanics and Technical Physics*, 2001, **42**(1):57~62

[11] Malik M R, Hypersonic flight transition data analysis using parabolized stability equations with chemistry effects. *J. Spacecraft. Rockets*, 2003, 40(3):332~344

[12] HHUANG Zhang-feng, CAO Wei, ZHOU Heng, The mechanism of breakdown in laminar-turbulent transition of a supersonic boundary layer on a flat plate-temporal mode, Science in China